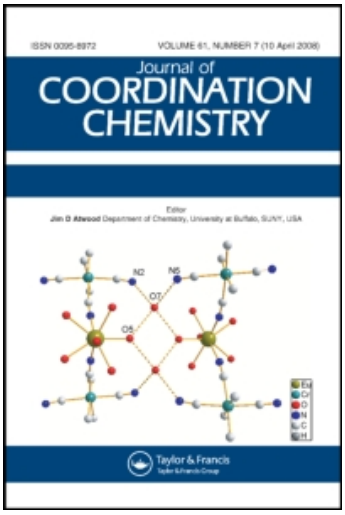

Journal of Coordination Chemistry
Publication details, including instructions for authors and subscription information:
http://www.informaworld.com/smpp/title~content=t713455674

Polydentate Schiff-base ligands and their Cd(II) and Cu(II) metal complexes: synthesis, characterization, biological activity and electrochemical properties

Mehmet Tümer[a]
[a] Faculty of Science and Arts, Chemistry Department, K. Maras Sütcü Imam University, Turkey

First published on: 11 June 2007

To cite this Article Tümer, Mehmet(2007) 'Polydentate Schiff-base ligands and their Cd(II) and Cu(II) metal complexes: synthesis, characterization, biological activity and electrochemical properties', Journal of Coordination Chemistry, 60: 19, 2051 — 2065, First published on: 11 June 2007 (iFirst)
To link to this Article: DOI: 10.1080/00958970701236727
URL: http://dx.doi.org/10.1080/00958970701236727

Journal of Coordination Chemistry
Vol. 60, No. 19, 1 October 2007, 2051–2065

Taylor & Francis
Taylor & Francis Group

Polydentate Schiff-base ligands and their Cd(II) and Cu(II) metal complexes: synthesis, characterization, biological activity and electrochemical properties

MEHMET TÜMER*

Faculty of Science and Arts, Chemistry Department, K. Maras Sütcü
Imam University, K. Maras 46100, Turkey

(*Received 3 October 2006; in final form 30 November 2006*)

Synthesis, characterization, microbiological activity and electrochemical properties of the Schiff-base ligands A^1–A^5 and their Cd(II) and Cu(II) metal complexes are reported. The ligands and their complexes have been characterized by elemental analysis, FT–IR, UV–Vis, ^{1}H- and ^{13}C-NMR, mass spectra, magnetic susceptibility and conductance measurements. In the complexes, all the ligands are bidentate, the oxygen in the *ortho* position and azomethine nitrogen atoms of the ligands coordinate to the metal ions. The keto-enol tautomeric forms of the Schiff-base ligands A^1–A^5 have been investigated in polar and non-polar organic solvents. Antimicrobial activity of the ligands and metal complexes were tested using the disc diffusion method and the chosen strains include *Bacillus megaterium* and *Candida tropicalis*. The electrochemical properties of the ligands A^1–A^5 and their Cu(II) metal complexes have been investigated at different scan rates (100–500 mV s^{-1}) in DMSO.

Keywords: Schiff bases; Antimicrobial activity; Electrochemical properties

1. Introduction

Condensation of primary amines with carbonyl compounds yields Schiff bases [1, 2]. Interest in transition metal complexes of Schiff bases [3–5] due to the fact that Schiff bases offer opportunities for inducing substrate chirality, tuning metal centered electronic factors, enhancing solubility and stability of either homogeneous or heterogeneous catalyst [6–11]. Schiff bases have been amongst the most widely studied coordination compounds and are becoming increasingly important as biochemical, analytical and antimicrobial reagents [12]. Schiff bases derived from a large number of carbonyl compounds and amines have been used [13, 14]. Schiff-base complexes derived from 4-hydroxysalicylaldehyde and amines have strong anticancer activity e.g. Ehrlich ascites carcinoma (EAC) [15]. It is well known that some drugs have increased activity when administered as metal complexes rather than as free organic compounds [16]. A large number of reports are available on the chemistry and the biological activities of transition metal complexes containing O, N and S, N donor atoms.

*Email: mtumer@ksu.edu.tr

Journal of Coordination Chemistry
ISSN 0095-8972 print/ISSN 1029-0389 online © 2007 Taylor & Francis
DOI: 10.1080/00958970701236727

The transition metal complexes having oxygen and nitrogen donor Schiff bases possess unusual configuration, structural liability and are sensitive to the molecular environment [16]. The environment around the metal center "as coordination geometry, number of coordinated ligands and their donor group" is the key factor for metalloproteins to carry out a specific physiological function [17]. Among different physicochemical properties of organic compounds, protonation and stability constants determined in mixed solvents provide an important basis for speculation about whether substituent effects influence their acidity and basicity. It also accepted that knowledge of the stability constants of such Schiff bases and their metal complexes may eventually help to throw light on the inactivation of essential trace metals in biological systems.

The present study deals with the preparation, characterization, antimicrobial activity and electrochemical properties of Schiff-base ligands and their metal complexes.

2. Experimental

2.1. *Materials*

All chemicals used in this study were obtained commercially and used without purification. 3,5-Di-tert-butyl-4-hydroxyaniline was prepared according to a known procedure [18].

2.2. *Physical measurements*

Elemental analyses (C, H, N) were performed using a Carlo Erba 1106 elemental analyser. Infrared spectra were obtained using KBr discs (4000–400 cm^{-1}) on a Shimadzu 8300 FT–IR spectrophotometer. Electronic spectra in the 200–900 nm range were obtained on a Shimadzu UV-160 A spectrophotometer. Magnetic measurements were carried out by the Gouy method using $Hg[Co(SCN)_4]$ as calibrant. Molar conductances of the Schiff-base ligands and their transition metal complexes were determined in DMSO ($\sim 10^{-3}$ M) at room temperature using a Jenway Model 4070 conductivity meter. Mass spectra of the ligands were recorded on a VG ZabSpec GC–MS spectrophotometer with fast atom bombardment. ^{1}H and ^{13}C NMR spectra were taken on a Varian XL-200 NMR instrument. TMS was used as internal standard and deuterated dimethyl sulfoxide as solvent. The metal content of the complexes were determined by an Ati Unicam 929 Model AA Spectrometer in solutions prepared by decomposing the compounds in aqua regia and then subsequently digesting in concentrated HCl.

Electrochemical studies were carried out with a Iviumstat Electrochemical workstation equipped with a low current module (BAS PA-1) at a platinum disk electrode and a platinum microelectrode of 10 μm diameter (BAS). Cyclic voltammetric measurements were made at room temperature in an undivided cell (BAS model C-3 cell stand) with a platinum counter reference electrode (BAS). All potentials are reported with respect to Ag/AgCl. The solutions were deoxygenated by passing dry nitrogen through the solution for 30 min prior to the experiments, and during the experiments N_2 flow was maintained over the solution. Digital simulations were performed using DigiSim 3.0 for windows (BAS, Inc.). Experimental cyclic voltammograms used for the fitting process had the background subtracted and were corrected electronically for Ohmic drop.

2.3. *Preparation of Schiff-base ligands (A^1–A^5)*

The Schiff-base ligands were prepared by condensing the amine derivatives (1 mmol; 0.172 g for *p*-bromaniline, 0.107 g for *p*-aminotoluene and 0.221 g for 3,5-di-tert-butyl-4-hydroxyaniline)) with carbonyl compounds (1 mmol; 0.154 g for 2,3,4-tri-hydroxybenzaldehyde, 0.138 g for 2,3- and 2,4-di-hydroxybenzaldehyde) in EtOH (40 mL) under reflux for 5–6 h. The precipitated ligand was filtered off, recrystallized from acetone/hexane (v/v) and dried in a vacuum desiccator.

2.4. *Preparation of Schiff-base complexes*

The appropriate quantity of Schiff base ligand (1 mmol) was dissolved in absolute EtOH (15 mL). To this solution, a solution of $Cd(ClO_4)_2 \cdot 6H_2O$ and $Cu(ClO_4)_2 \cdot 6H_2O$ (0.5 mmol) in absolute EtOH (15 mL) [1 : 2 molar ratio, M : L] was added. The mixture was stirred for 3 h at 80°C. The precipitated complex was then filtered off, washed with cold ethanol and dried in a vacuum dessicator.

Caution: As perchlorate salts may be explosive, they must be handled carefully.

2.5. *Preparation of microbial culture*

Fourteen compounds were evaluated for their *in vitro* antibacterial activity against *Bacillus megaterium* DSM 32 and antifungal activity against *Candida tropicalis* FMC 23 by agar-well diffusion. Bacterium was inoculated into Nutrient Broth (Difco) and incubated for 24 h and the fungi studied inculated in Malt Extract Broth (Difco) for 48 h. In the agar-well diffusion method, Mueller Hinton Agar (Oxoid) for bacterium and in Malt Extract Broth (Difco) sterilized in a flask and cooled to 45–50°C was distributed (20 mL) to sterilized petri dishes after injecting 0.01 mL cultures of bacterium prepared as mentioned above and allowed to solidify. The dilution plate method was used to enumerate microorganisms (10^5 bacterium mL^{-1}) and fungi (10^3–10^4 mL^{-1}) for 24 h [19]. By using a sterilised cork borer (7 mm diameter), wells were dug in the culture plates. Compounds dissolved in $CHCl_3$ were added (0.2 µL) to these wells. The petri dishes were left at 4°C for 2 h and then the plats were incubated at 30°C for bacterium (18–24 h) and at 25°C for fungi (72 h). At the end of the period, inhibition zones formed on the medium were evaluated is millimeters (mm). The control samples were only absorbed in $CHCl_3$.

3. Results and discussion

The ligands 4-[(4-bromo-phenylimino)-methyl]-benzene-1,2,3-triol (A^1), 4-[(3,5-di-tert-butyl-4-hydroxy-phenylimino)-methyl]-benzene-1,2,3-triol (A^2), 3-(*p*-tolylimino-methyl)-benzene-1,2-diol (A^3), 3-[(4-bromo-phenylimino)-methyl]-benzene-1,2-diol (A^4) and 4-[(3,5-di-tert-butyl-4-hydroxy-phenylimino)-methyl]-benzene-1,3-diol (A^5) and their Cu(II) and Cd(II) complexes have been synthesized and the substituent effects

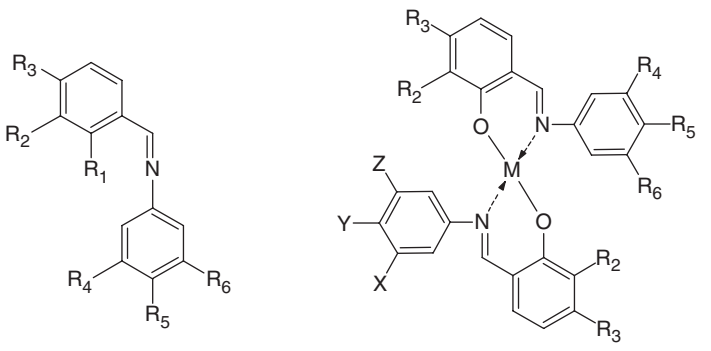

M: Cu(II) and Cd(II)

Ligand	R^1	R^2	R^3	R^4	R^5	R^6
A^1	OH	OH	OH	H	Br	H
A^2	OH	OH	OH	$(CH_3)_3C$	OH	$(CH_3)_3C$
A^3	OH	OH	H	H	CH3	H
A^4	OH	OH	H	H	Br	H
A^5	OH	H	OH	$(CH_3)_3C$	OH	$(CH_3)_3C$

Figure 1. Proposed structures of the ligands and their metal complexes.

on the electronic properties discussed. The proposed structures of the ligands and their metal complexes are shown in figure 1.

Condensation of the aldehydes with primary amines readily gives the corresponding imines, which were easily identified by their IR, ^{1}H- and ^{13}C-NMR spectra. Replacement of the carbonyl by the imine results in: (i) lowering of the energy of the ν(C=O) stretch in the IR spectrum and (ii) a shift to higher field of the CH=N proton signal in the ^{1}H-NMR spectrum. The imines prepared in this way are formed in nearly quantitative yields and are of high purity. All compounds, except 3,5-di-tert-butyl-4-hydroxyaniline, are very stable at room temperature in the solid state. The electron withdrawing or –attracting groups at the *ortho* and *para* positions of the ligands produce different electronic and steric effects. Therefore, it may be possible that the tert-butyl groups on the aniline ring and the hydroxy group *meta* to OH in the salicylidene moiety lead to a decrease in stability of the complexes. The yields of the complexes are lower than the ligands. Further stirring and heating did not increase the yield of the complexes containing tert-butyl groups. The low yields may be due to steric hindrance around the coordination center. All the ligands and their complexes are soluble in common organic solvents such as $CHCl_3$, EtOH, MeOH, THF, etc. Solution conductivity measurements were performed to establish the charge of the complexes. The results show that all compounds are non-electrolytes [20]. The results of the elemental analyses, given in table 1, are in good agreement with suggested compositions of ligands and their metal complexes.

The infrared spectral data of the ligands (A^1–A^5) and their metal complexes are given in table 2. In the infrared spectra of ligands A^2 and A^5, the strong vibration at 3610 and

Table 1. Some analytical and physical data for the imine ligands and their complexes.

Compound	Color	μ_{eff} (as BM)	Yield (%)	M.p. (°C)	Found (Calcd)% C	N	H	M	$^{a}\Lambda_M$
A^1	Orange	–	84	201	50.60(50.65)	4.57(4.55)	3.22(3.25)	–	1.8
$Cu(A^1)_2$	Brown	1.79	74	>250	46.09(46.05)	4.17(4.13)	2.63(2.66)	9.45(9.38)	7.4
$Cd(A^1)_2$	Light orange	Diamag.	70	>250	42.98(42.95)	3.87(3.85)	2.51(2.48)	15.55(15.47)	7.0
A^2	Yellow	–	85	204	70.56(70.59)	3.88(3.92)	7.53(7.56)	–	1.2
$Cu(A^2)_2$	Dark brown	1.80	60	>250	65.03(64.99)	3.64(3.61)	6.74(6.71)	8.19(8.27)	6.8
$Cd(A^2)_2$	Yellow	Diamag.	70	>250	61.16(61.13)	3.36(3.40)	6.34(6.31)	13.72(13.64)	9.0
A^3	Orange	–	87	156	74.04(74.01)	6.15(6.17)	5.69(5.73)	–	1.5
$Cu(A^3)_2$	Light brown	1.81	68	>250	65.20(65.17)	5.46(5.43)	4.70(4.66)	12.40(12.32)	6.9
$Cd(A^3)_2$	Orange	Diamag.	79	238	59.50(59.53)	5.01(4.96)	4.28(4.25)	19.99(19.91)	8.0
A^4	Orange	–	90	184	53.56(53.42)	4.83(4.79)	3.47(3.42)	–	1.0
$Cu(A^4)_2$	Dark brown	1.80	65	>250	48.30(48.33)	4.32(4.34)	2.83(2.79)	9.90(9.84)	8.5
$Cd(A^4)_2$	Orange	Diamag.	65	201[d]	44.89(44.93)	4.04(4.03)	2.64(4.59)	16.26(16.19)	10.0
A^5	Yellow	–	86	163	73.87(73.90)	4.16(4.11)	7.88(7.92)	–	1.9
$Cu(A^5)_2$	Dark brown	1.81	70	>250	67.81(67.78)	3.74(3.77)	7.02(6.99)	8.65(8.55)	7.3
$Cd(A^5)_2$	Light yellow	Diamag.	68	124[d]	63.58(63.60)	3.57(3.53)	6.60(6.56)	14.27(14.19)	7.6

[a] $\Omega^{-1}\,cm^2\,mol^{-1}$. [d] Decompose.

3600 cm^{-1} can be attributed to the free hydroxy group on the aniline moiety. In the complexes, these bands are seen at the same region. In the ligands, bands in the 3450–3375 cm^{-1} range may be assigned to ν(O–H) stretching on the salicylidene moiety. For the free ligands, the broad bands in the 2800–2700 cm^{-1} range are assigned to the OH group vibration (*ortho* position) associated intramolecularly with the nitrogen atom of the CH=N group [21]. These bands disappear in the complexes, as a result of proton substitution by cation coordination to oxygen. For the ligands, the strong bands observed in the 1641–1620 cm^{-1} range are assigned to the azomethine group vibration. These bands are slightly shifted towards lower frequencies in the complexes, and this change in the frequncies shows that the imine nitrogen atom coordinates to the Cd(II) and Cu(II) ions. The medium intensity bands observed for all ligands in the 1300–1265 cm^{-1} range can be attributed to the phenolic stretch. These bands are observed at lower wavenumber by ca 10–20 cm^{-1} relative to the free ligands for the complexes suggesting involvement of the oxygen atom of the C–O moiety in coordination [22]. In all of the complexes a medium and/or weak band observed in the 480–510 and 415–448 cm^{-1} range can be attributed to the ν(M–O) and ν(M–N) [23] modes, respectively.

In the case of the ligands and their metal complexes, it is particularly important to establish whether the molecules retain the imine character of their phenol precursor. The most useful techniques to investigate the tautomeric forms (figure 2) of these ligands are UV and NMR spectroscopy, while IR seems of limited value here because location of the ν(C=O) and ν(C–O) stretches in the spectra is obscured by the abundance of aromatic skeletal modes. In order to investigate the keto-enol tautomeric forms of the free ligands, the electronic spectra were measured in heptane, chloroform and ethanol. In heptane, the ligands exhibit maxima in the 320–278 nm range. However, in chloroform and ethanol, new bands in the 464–317 nm range were observed. The former set (~278 nm) in heptane has been assigned to the enolimine tautomer and the latter to the ketoamine tautomer of the Schiff bases [24].

Table 2. Infrared[a] and electronic spectral data for the Schiff-base ligands and their metal complexes (cm^{-1}).

Compounds	ν(OH)^x	ν(OH)	ν(CH$_3$)^y	ν(O–H $\cdots$ N)	ν(CH=N)	ν(C–OH)	ν(M–O)	ν(M–N)	λ_{max} (nm)
A^1	–	3450 br	–	2800 m	1620 s	1290	–	–	420, 375, 339, 280, 240
A^2	3610 s	3380 br	2980 s	2790 m	1620 s	1280	–	–	425, 348, 294, 255
A^3	–	3400 br	2910 s	2700 m	1641 s	1283	–	–	359, 320, 281, 226
A^4	–	3375 br	–	2745 m	1633 s	1300	–	–	464, 368, 317, 279, 271
A^5	3600 s	3410 br	2975 s	2740 m	1625 s	1265	503 w	434 w	430, 275, 225
$Cd(A^1)_2$	–	–	–	–	1605 m	1270	505 w	428 w	418, 354, 287, 238
$Cd(A^2)_2$	3608 s	–	2978 s	–	1610 m	1276	497 w	415 w	357, 289, 234
$Cd(A^3)_2$	–	–	2910 s	–	1614 s	1275	500 w	434 w	389, 334, 271, 245, 220
$Cd(A^4)_2$	–	–	–	–	1620 s	1294	503 w	444 w	438, 354, 305, 262, 260
$Cd(A^5)_2$	3600 s	–	2975 s	–	1613 s	1260	510 w	424 w	422, 354, 349, 283, 238
$Cu(A^1)_2$	–	–	–	–	1612 s	1275	490 w	448 w	624, 380, 324, 275, 216
$Cu(A^2)_2$	3609 s	–	2977 s	–	1618 s	1273	480 w	442 w	633, 412, 285, 254, 215
$Cu(A^3)_2$	–	–	2909 s	–	1613 s	1270	495 w	420 w	610, 370, 341, 295, 271, 227
$Cu(A^4)_2$	–	–		–	1624 s	1250	497 w	430 w	612, 363, 325, 294, 270,221
$Cu(A^5)_2$	3598 s	–	2975 s	–	1610 s	1262	485 w	418 w	627, 429, 327, 220

[a]br (broad), s (strong), m (medium), w (weak). *x*: sterically hindered phenol, *y*: CH_3 on the ligand A^3 and CH_3 group of the tert-butyl groups on the ligands A^2 and A^5.

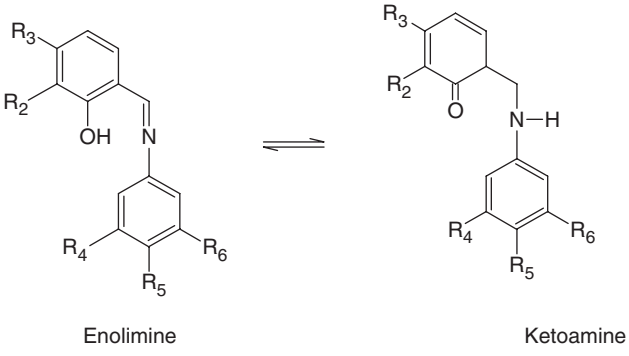

Figure 2. Keto-enol tautomerism forms of the bidentate A^1–A^5 Schiff-base ligands.

Electronic spectra have been measured in EtOH and the numerical data are given in table 2. Hydrogen-bonding solvents (EtOH) thus favour the formation of the ketoamine. The interaction of enolimine with a hydrogen bond forming solvent would presumably reduce the O–H bond strength and facilitate proton transfer to the nitrogen centre. In like manner, the bands in the 464–337 nm range are also assigned to n–π^* transition of the azomethine group. In the spectra of the complexes, the bands of the azomethine n–π^* transition are shifted to lower frequencies indicating that the imine nitrogen atom is involved in coordination to the metal ion. The bands at higher energies (~290–215 nm range) are associated with benzene π–π^* transitions. The spectra of the complexes show intense bands in the high-energy region at 305–370 nm which can be assigned to charge transfer $L \rightarrow M$ bands [25]. Although the precise nature of this transition involving the phenolate group is not clear [it has been considered to be an O(phenolate) $\rightarrow$ metal(II) LMCT [26] or as a metal(II) $\rightarrow \pi^*$ (phenolate) MLCT [27] transition], it is agreed that a higher energy component should exist near 330 nm [26]. tert-Butyl groups on the aniline occupy a more significant region of space in the vicinity of the metal centre due to the presence of the branched carbon. Therefore, it is quite plausible that a sterically induced increase in the average metal-ligand separation results in a hypsochromic shift in the CT absorption maximum. The spectra of the Cu(II) complexes contain one absorption band in the 633–610 nm range which may be assigned to the d–d transition of the Cu(II) ion suggesting that they are four-coordinate complexes.

Magnetic measurements were recorded at room temperature and the effective magnetic moment (μ_{eff}) values of the complexes are shown in table 1. The magnetic moments of the copper(II) complexes were observed in the range of 1.79–1.81 B.M. which corresponds to a single unpaired electron with a very slight orbital contribution consistent with square-planar geometry [28]. The structures of the monomeric complexes are supported by magnetic moment data. The Cd(II) complexes of the ligands A^1–A^5 are diamagnetic with tetrahedral geometry.

Additional structural information can be deduced from the ^{1}H- and ^{13}C-NMR spectra. The ^{1}H- and ^{13}C-chemical shifts for the Schiff-base ligands are given in table 3. The ^{1}H- and ^{13}C-NMR spectra of A^5 is shown in figure 3. The influence of substitution on the chemical shifts of the aniline moiety is weak. When the bromo is present on

Table 3. The ^1H (^{13}C) NMR data (as ppm) for the Schiff-base ligands using $CDCl_3$ as solvent.

Ligands	CH_3	*t*-Bu	Ar	CH=N	OH
A^1	–	–	7.20–7.74 (112.81–152.45)	8.94 (163.15)	10.45–11.70
A^2	–	1.51 (32.00)	7.14–7.19 (110.10–156.66)	8.38 (166.75)	10.10–12.15
A^3	2.28 (27.30)	–	7.18–7.60 (116.13–157.17)	8.90 (162.52)	10.60–11.05
A^4	–	–	7.32–7.72 (113.40–154.61)	8.92 (165.05)	10.55, 10.30
A^5	–	1.62 (32.95)	7.04–7.29 (115.20–155.00)	8.39 (169.90)	10.10–12.30

CH_3 coupling constant $J \sim 3$ Hz.

the aniline, a significant deshielding of the proton signals can be observed, due to the strong electron-withdrawing effect. However, the OH groups on the salicylidene moiety increase the electron density of the aromatic rings, due to the resonance or mesomeric effect. In Schiff-base ligands A^1–A^5, there is the proton donor OH and one proton acceptor in the *ortho* position. The ^1H resonance of the O–H group in the 10.10–12.30 ppm range disappears in D_2O.

Formulations of the ligands are deduced from analytical data, ^1H- and ^{13}C-NMR and further supported by mass spectroscopy. The relatively low intensities of the molecular ion peaks, $[M]^+$, are indicative of the ease of fragmentation of the compounds, and this reflects the number of heteroatoms present in each structure. The spectra of the ligands A^1–A^5 show peaks at *m*/*e* 308, 357, 227, 292 and 341 $[M]^+$, respectively. All the ligands decompose similarly.

The free ligands and their metal complexes were tested against the *B. megaterium* and *C. tropicalis*. The diffusion method was used to evaluate the antimicrobial activities of the tested compounds and the results are given in table 4. The antibacterial results showed that some metal complexes are more toxic to *B. megaterium* and *C. tropicalis* than free ligands. This is due to chelation, which reduces the polarity of the metal atom because of partial sharing of its positive charge with the donor groups and possible π-electron delocalization within the whole chelate ring. Chelation also increases the lipophilic nature of the central atom which subsequently favors its permeation through the lipid layer of the cell membrane [29]. Complexes $Cu(A^2)_2$ and $Cu(A^5)_2$ show the highest activity against *C. tropicalis*.

The redox properties of the ligands and their metal complexes were investigated in DMSO solution (in nitrogen atmosphere) by cyclic voltammetry (table 5) in the potential range +2.0 to −2.0 V. The cyclic voltammograms have been recorded at a wide range of scan rates from 100 to 500 mV s^{-1}. The cyclic voltammograms of the ligands A^3 and A^5 (figures 4 and 5) show the ligands have cathodic and anodic peaks. In the scan rate 100 mV s^{-1}, for the Schiff-base ligands A^1, A^3 and A^4, consist of a single cathodic peak at potentials ranging from −0.360–0.710 V; anodic wave occurs at potentials ranging from −0.900–0.320 V in the reverse scan. Such a reduction process should correspond to a totally irreversible electron transfer, but in the scan rate 500 mV s^{-1}, the same ligands have more positive and negative potentials. This situation shows that the scan rate affects the cathodic and anodic potentials. In other words, the ligands A^2 and A^5 have two anodic and cathodic peaks. These peaks are in the range

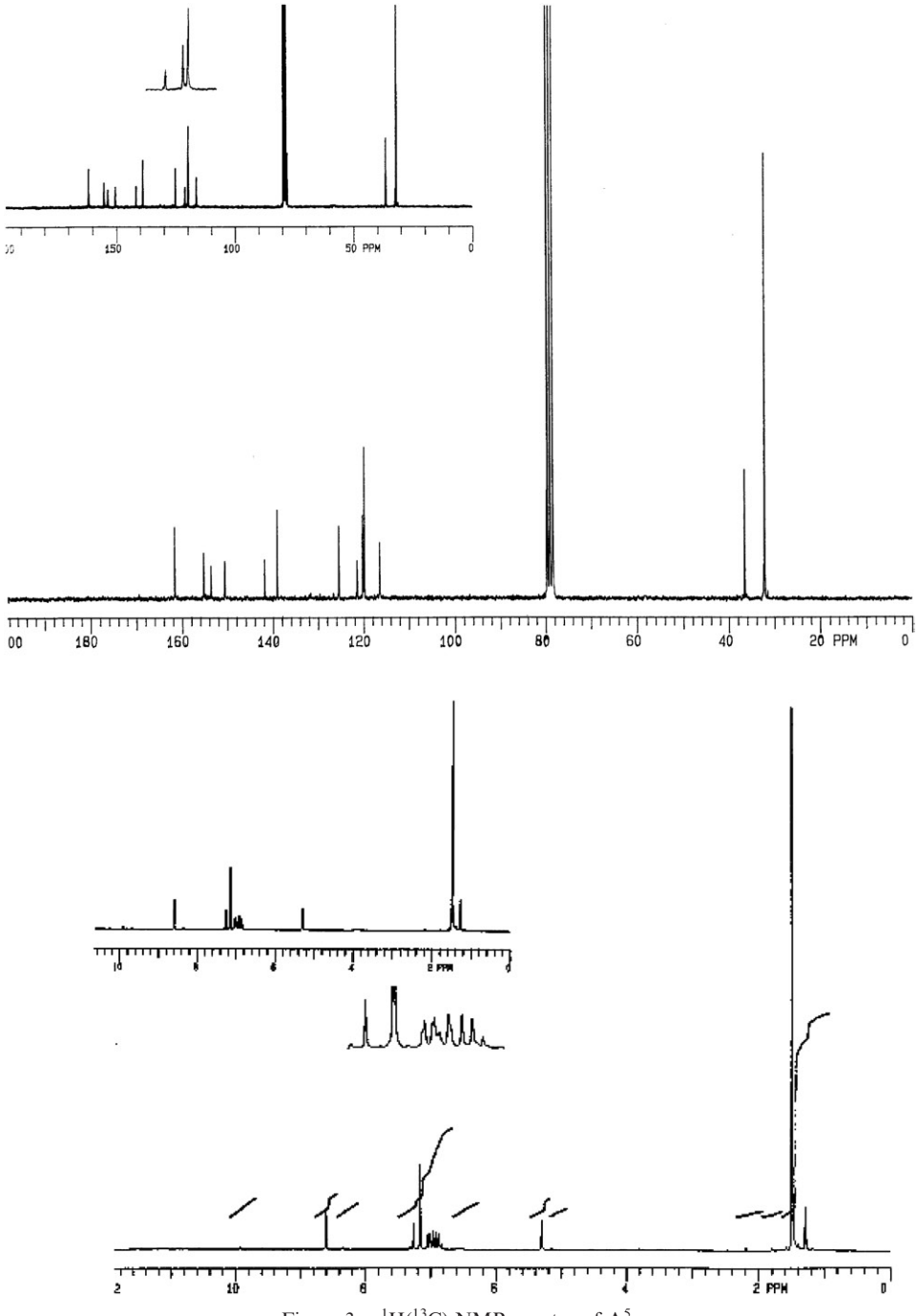

Figure 3. $^{1}H(^{13}C)$-NMR spectra of A^{5}.

Table 4. Antimicrobial effects of the ligands and their metal complexes.[a]

Compound	Inhibition zone (mm[b]) *C. tropicalis*	Inhibition zone (mm[b]) *B. megaterium*
Control ($CHCl_3$)	–	–
A^1	15	18
A^2	10	14
A^3	7	12
A^4	13	13
A^5	12	15
$Cd(A^1)_2$	18	23
$Cd(A^2)_2$	17	21
$Cd(A^3)_2$	11	20
$Cd(A^4)_2$	13	18
$Cd(A^5)_2$	24	21
$Cu(A^1)_2$	15	19
$Cu(A^2)_2$	26	22
$Cu(A^3)_2$	21	17
$Cu(A^4)_2$	23	20
$Cu(A^5)_2$	26	18

[a]Conc. of compounds is 50 μg cm^{-3}. [b]Including diameter of disc (6 mm).

Table 5. Electrochemical data of the Schiff-base ligands and their complexes.

Compounds	E_{pa} (V)	E_{pc} (V)	$E_{1/2}$ (mV)	ΔE_p(mV)
A^1	−0.560	0.680	60	−1240
	[−0.750]*	[0.960]*		
$Cu(A^1)_2$	−0.620, −0.100	0.860	120	−1440
	[−0.970, 0.260]*	[−0.670]*		
A^2	−0.290, 0.460	−0.360, 0.320	390	140
	[−0.185, 0.450]*	[−0.225, 0.680]*		
$Cu(A^2)_2$	−0.240	0.810	285	−1050
	[−0.660]*	[0.510]*		
A^3	−0.900	−0.240	−570	−660
	[−1.030]*	[−0.470]		
$Cu(A^3)_2$	−1.360, −0.190	−0.590	−975	−770
	[−0.210, 0.520]*	[−0.980, 1.070]*		
A^4	−0.880	0.710	−85	1590
	[−0.900]*	[0.980]*		
$Cu(A^4)_2$	−1.410, −0.420	0.680	365	2090
	[−0.740]*	[−0.150]*		
A^5	−0.340, 0.640	−0.440, 0.480	−390	100
	[−0.250, 0.670]*	[−0.410, 0.710]*		
$Cu(A^5)_2$	−1.450, −0.620	0.900	−275	−2350
	[−0.710, 0.750]*	[0.680]*		

Supporting electrolyte: $[NBu_4](ClO_4)$ (0.05 M); concentrations of the compounds: 0.001 M. All the potentials are referenced to Ag/AgCl; where E_{pa} and E_{pc} are anodic and cathodic potentials, respectively. $E_{1/2} = 0.5 \times (E_{pa} + E_{pc})$, $\Delta E_p = E_{pa} - E_{pc}$. []*: These data have been obtained from 500 mV s^{-1} scan rate. Other data have been obtained at 100 mV s^{-1} scan rate.

−0.225–0.710 V for cathodic peaks and −0.185–0.670 V for anodic peaks. As seen from figures 5–6, there are two oxidation and reduction peaks, indicating this redox process is reversible. In this reaction, the quinone structure has been formed (figure 6). Such a process would involve self-protonation reactions where the phenolic hydroxyl groups act as proton donors. In complexes of A^2 and A^5, this is not observed (figure 7).

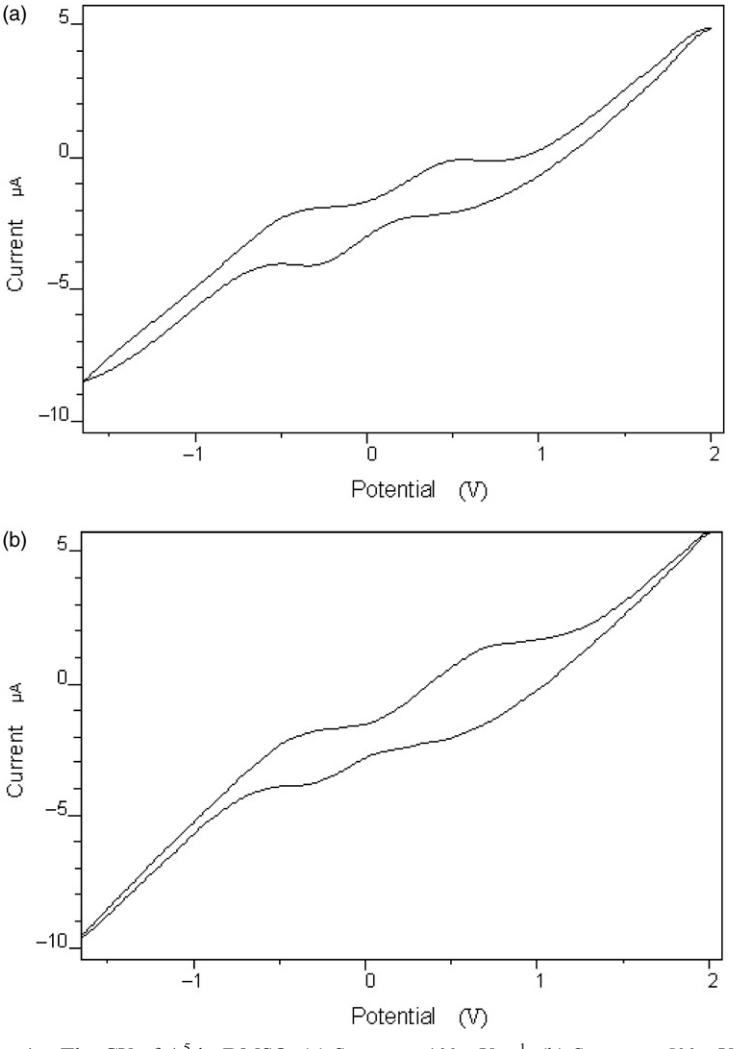

Figure 4. The CV of A^5 in DMSO. (a) Scan rate 100 mV s^{-1}. (b) Scan rate 500 mV s^{-1}.

In each series of ligands, the cathodic peak potential (E_{pc}) corresponding to the intramolecular reductive coupling of the imine groups varies as can be expected from the electronic effects of the substituents at positions 2,2′ and 3,3′. Thus, in the ligands, E_{pc} becomes more negative according to the sequence OH, OCH_3, CH_3 and Br, i.e. in order of an increase in both electron-withdrawing and acceptor qualities of the substituents. This agrees with a mechanism involving self-protonation reactions for the electrochemical reduction of the imine groups in the Schiff-base ligands in the study.

Electrochemical studies of the Cu(II) complexes of A^1–A^5 were performed using DMSO as the solvent and tetrabutylammonium perchlorate as the supporting electrolyte at a scan rate of 100 and 500 mV s^{-1}. Typical cyclic voltammetry (CV) behavior of $Cu(A^{3-5})_2$ are shown in figures 7–9. The cyclic voltammograms of the

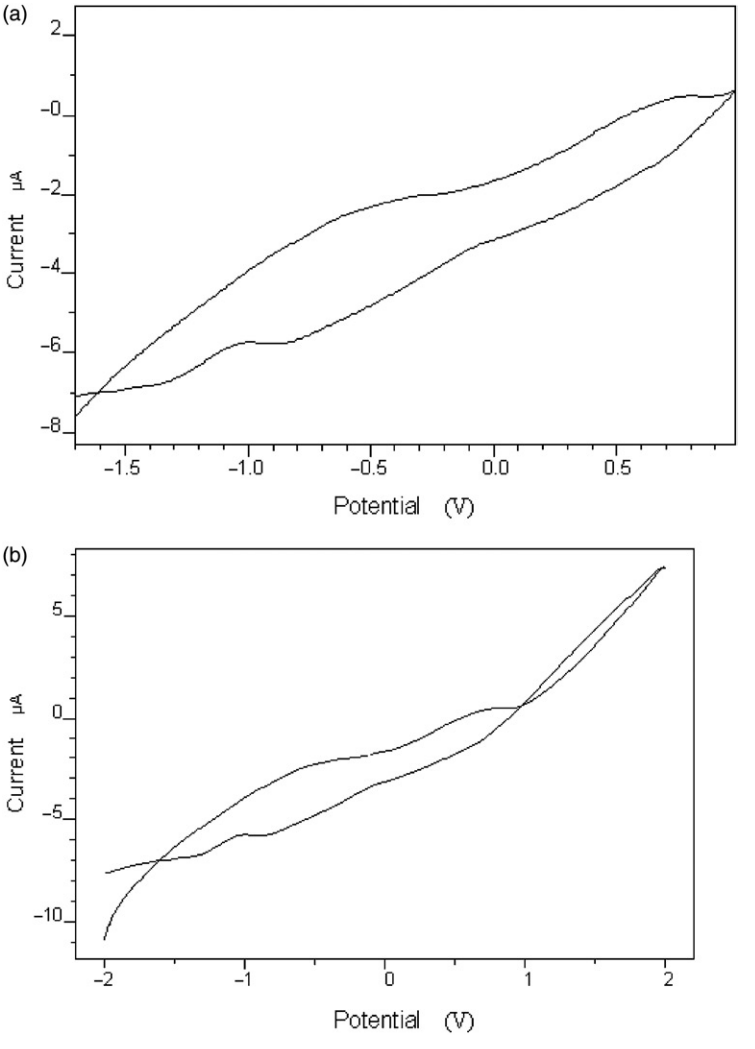

Figure 5. The CV of A^3 in DMSO. (a) Scan rate 100 mV s^{-1}. (b) Scan rate 500 mV s^{-1}.

$Cu(A^1)_2$ and $Cu(A^{3-5})_2$ complexes featured two anodic peaks ($E_{pa1} = -1.450$–0.240 V for 100 mV s^{-1} and $-0.970-(-0.210)$ V for 500 mV s^{-1}; and $E_{pa2} = -0.620-(-0.100)$ V *versus* Ag/AgCl) and one cathodic peak, except the $Cu(A^1)_2$ and $Cu(A^3)_2$ complexes, ($E_{pc1} = -0.980$–1.070 V *versus* Ag/AgCl). In other words, the $Cu(A^2)_2$ complex shows one anodic and cathodic peak ($E_{pa1} = -0.240$ V for 100 mV s^{-1}; and -0.660 V *versus* Ag/AgCl for 500 mV s^{-1}). The oxidation of Cu(0)/Cu(I)(E_{pa1}) is an irreversible process. The oxidation peak E_{pa2} belongs to Cu(I)/Cu(II), and reduction of Cu(II) occurred, upon scan reversal at 0.520 V. The separation of the anodic and cathodic peak potentials, $E_p = 100$ mV, and the ratio of anodic to cathodic peak currents, $i_{pa}/i_{pc} = 1.54$, indicate a quasi-reversible redox process. The formal potential $E_{1/2}$, taken as average of E_{pc} and E_{pa} is 461.5 mV. The other cathodic peak E_{pc2} may be caused by the absorption of Cu(I) to the surface of the electrode, and gives the

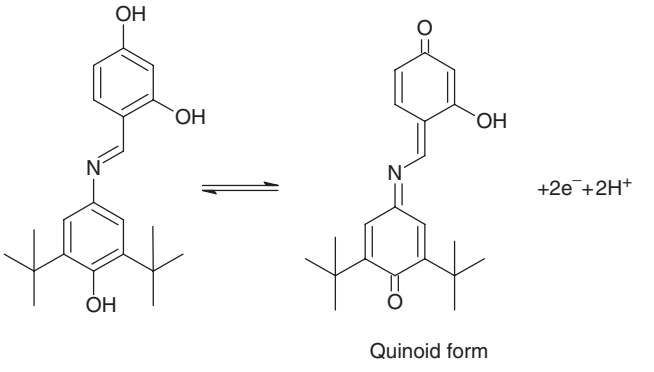

Figure 6. Redox process of A^5.

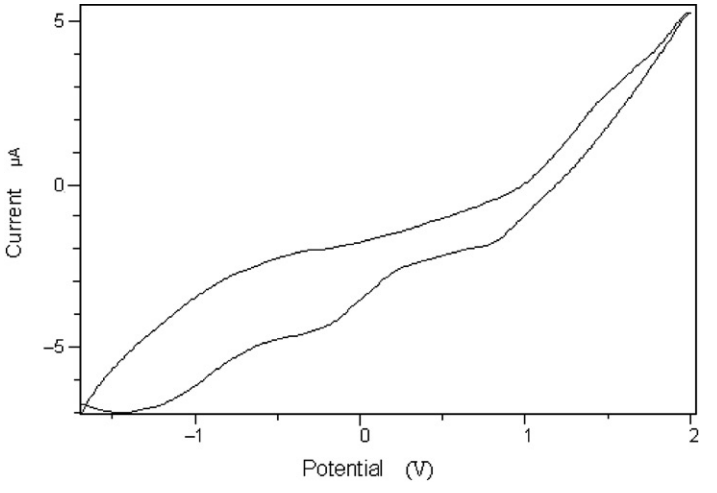

Figure 7. The CV of $(A^5)_2Cu$ in DMSO. Scan rate 100 mV s^{-1}.

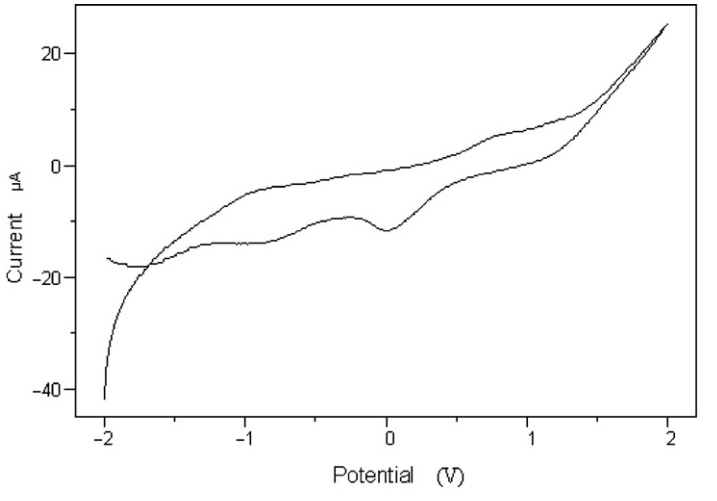

Figure 8. The CV of $(A^4)_2Cu$ in DMSO. Scan rate 100 mV s^{-1}.

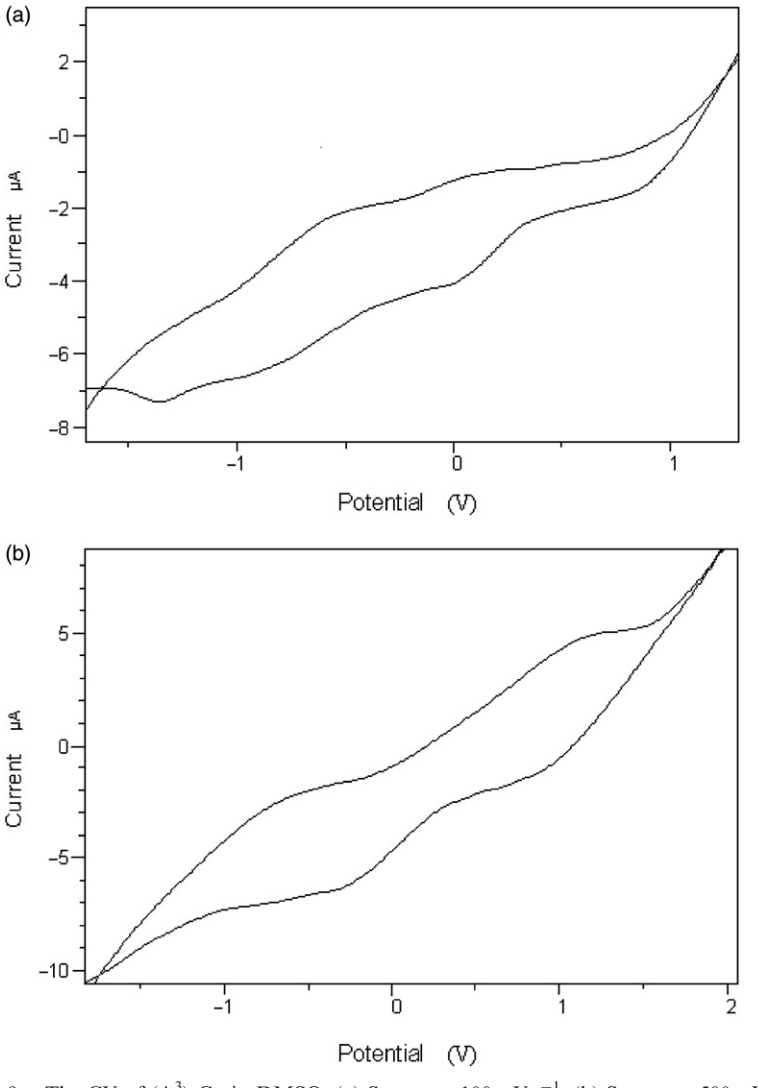

Figure 9. The CV of $(A^3)_2Cu$ in DMSO. (a) Scan rate 100 mV s^{-1}. (b) Scan rate 500 mV s^{-1}.

forward peak. The voltammogram also shows a broad cathodic peak at −1.1 V with an anodic counter at −0.1 V, possibly due to the Cu(I)/Cu(0) couple. The reduced Cu(0) is absorbed on the electrode surface as evidenced from the narrow width of the anodic response with a large peak current. On carrying out the experiment with back scan going to negative potential to −0.6 V does not show such large anodic current at −0.1 V.

Acknowledgement

I wish to thank Dr Metin Dığrak (K. Maras Sutcu Imam University, Biology Department) for the antimicrobial activity studies.

References

[1] N. Geeraert, H. Schiff. *Z. M. Neue*, **143**, 59 (1982).
[2] K. Dey, A.K. Biswas, A. Roy. *Indian J. Chem. A*., **20**, 848 (1981).
[3] K.S. Murray. *Aust. J. Chem*., **58**, 203 (1978).
[4] H. Doine. *Bull. Chem. Soc. Jpn*, **58**, 1327 (1985).
[5] K. Nakajima, Y. Ando, H. Mano, M. Kojima. *Inorg. Chim. Acta*, **274**, 184 (1998).
[6] B. De Clercq, F. Verpoort. *Macromolecules*, **35**, 8943 (2002).
[7] T. Opstal, F. Verpoort. *Angew. Chem. Int. Edit*., **42**, 2876 (2003).
[8] T. Opstal, F. Verpoort. *Synlett*, **6**, 935 (2002).
[9] S.N. Pal, S. Pal. *Inorg. Chem*., **40**, 4807 (2001).
[10] B. De Clercq, F. Verpoort. *Adv. Synth. Catal*., **34**, 639 (2002).
[11] B. De Clercq, F. Lefebvre, F. Verpoort. *Appl. Catal. A*, **247**, 345 (2003).
[12] M. Tümer, H. Köksal, M.K. Şener, S. Serin. *Trans. Met. Chem*., **24**, 414 (1999).
[13] J.W. Pyrz, A.I. Roe, L.J. Stern, J.R. Que. *J. Am. Chem. Soc*., **107**, 614 (1985).
[14] M. Tümer, B. Erdoğan, H. Köksal, S. Serin, M.Y. Nutku. *Synth. React. Inorg. Met.-Org. Chem*., **28**, 529 (1998).
[15] W. Zishen, L. Zhiping, Y. Zhenhuan. *Trans. Met. Chem*., **18**, 291 (1993).
[16] J. Chakraborty, R.N. Patel. *J. Indian Chem. Soc*., **73**, 191 (1996).
[17] R. Klement, F. Stock, H. Elias, H. Paulus, P. Pelikan, M. Valko, M. Muzur. *Polyhedron*, **18**, 3617 (1999).
[18] A. Rieker, K. Scheffler, R. Mayer, E. Müler. *B. Narr. Ann*., **10**, 693 (1966).
[19] C.H. Collins, P.M. Lyne, J.M. Grange. *Microbiological Methods*, 6th Edn, p. 410, Butterworth & Co., Oxford (1989).
[20] W.J. Geary. *Coord. Chem. Rev*., **7**, 81 (1971).
[21] M. Dolaz, M. Tümer. *Trans. Met. Chem*., **29**, 516 (2004).
[22] M. Tümer, C. Çelik, H. Köksal, S. Serin. *Trans. Met. Chem*., **24**, 525 (1999).
[23] M. Dolaz, M. Tümer, M. Dığrak. *Trans. Met. Chem.* (In press).
[24] M. Tümer. *Synth. React. Inorg. Met.-Org. Chem*., **30**, 1139 (2000).
[25] R. Atkins, G. Brewer, E. Kokot, G.M. Mockler, E. Sinn. *J. Inorg. Chem*., **24**, 127 (1985).
[26] A. Garnier-Suillerot, J.P. Albertini, A. Collet, L. Faury, J.M. Pastor, L.J. Tosi. *J. Chem. Soc. Dalton Trans*., 2544 (1981).
[27] A.R. Amundsen, J. Whelan, B. Bosnich. *J. Am. Chem. Soc*., **99**, 6730 (1977).
[28] H. Köksal, M. Dolaz, M. Tümer, S. Serin. *Synth. React. Inorg. Met.-Org. Chem*., **31**, 1141 (2001).
[29] N. Fahmi, I.J. Gupta, R.V. Singh. *Phosphorus Sulfur Silicon*, **132**, 1 (1998).